Title 論文題目	Preservation of interhemispheric cortical connections through corpus callosum following intravenous infusion of mesenchymal stem cells in a rat model of cerebral infarction (ラット脳梗塞モデルに対する骨髄間葉系幹細胞の経静脈的移植後に惹起される脳梁を介する大脳半球間皮質連絡の保護)
Author(s) 著　者	長濱，宏史
Degree number 学位記番号	甲第 3018 号
Degree name 学位の種別	博士（医学）
Issue Date 学位取得年月日	2018-03-31
Original Article 原著論文	札幌医学雑誌　第 87 巻　第 1 号（平成 31 年 3 月）掲載予定
Doc URL	
DOI	
Resource Version	Author Edition

Preservation of interhemispheric cortical connections through corpus callosum following intravenous infusion of mesenchymal stem cells in a rat model of cerebral infarction

Hiroshi Nagahama, BS [1]; Masahito Nakazaki, MD, PhD [1]; Masanori Sasaki, MD, PhD [1, 2, 3]; Yuko Kataoka-Sasaki, MD, PhD [1]; Takahiro Namioka, MD; Ai Namioka, MD, Shinichi Oka, MD, PhD [1]; Rie Onodera, PhD [1]; Junpei Suzuki, PhD [1]; Yuichi Sasaki, PT, PhD [1]; Jeffery D. Kocsis, PhD [2, 3]; Osamu Honmou, MD, PhD [1, 2, 3]

[1] Department of Neural Regenerative Medicine, Research Institute for Frontier Medicine, Sapporo Medical University School of Medicine, Sapporo, 060-8556, Japan

[2] Department of Neurology, Yale University School of Medicine, New Haven, Connecticut, 06510, USA

[3] Center for Neuroscience and Regeneration Research, VA Connecticut Healthcare System, West Haven, Connecticut, 06516, USA

Key Words: transplantation, mesenchymal stem cell, stroke

Running head: Intravenous infusion of MSCs into a brain stem infarction

Number of words in the abstract: 216

Number of words in the text: 3773

Number of figures: 7

Address for correspondence:

Masanori Sasaki M.D., Ph.D.

Department of Neural Regenerative Medicine, Research Institute for Frontier Medicine,

Sapporo Medical University School of Medicine,

Sapporo, Hokkaido, 060-8556, Japan

TEL: +81-11-611-2111 (ext. 25070)

FAX: +81-11-616-3112

E-mail: msasaki@sapmed.ac.jp

Abstract

Systemic administration of mesenchymal stem cells (MSCs) following cerebral infarction exerts functional improvements. Previous research has suggested potential therapeutic mechanisms that promote neuroprotection and synaptogenesis. These include secretion neuroprotection, remodeling of neural circuits, restoration of the blood brain barrier, reduction of inflammatory infiltration and demyelination, and elevation of trophic factors. In addition to these mechanisms, we hypothesized that restored interhemispheric bilateral motor cortex connectivity might be an additional mechanism of functional recovery. In the present study, we have shown, with both MRI diffusion tensor imaging (DTI) and neuroanatomical tracing techniques using an adeno-associated virus (AAV) expressing GFP, that there was anatomical restoration of cortical interhemispheric connections through the corpus callosum after intravenous infusion of MSCs in a rat middle cerebral artery occlusion (MCAO) stroke model. Moreover, the degree of connectivity was greater in the MSC-treated group than in the vehicle-infused group. In accordance, both the thickness of corpus callosum and synaptic puncta in the contra-infarcted motor cortex connected to the corpus callosum were greater in the MSC-treated group than in the vehicle group. Together, these results suggest that distinct preservation of interhemispheric cortical connections through corpus callosum was promoted by intravenous infusion of MSCs. This anatomical preservation of the motor cortex in the contra-infarcted hemisphere may contribute to functional improvements following MSC therapy for cerebral stroke.

Highlights

- Interhemispheric cortical connections through corpus callosum after intravenous infusion of mesenchymal stem cells in stroke were shown using both DTI and AAV-based GFP tracing techniques.
- The degree of interhemispheric neural fibers shown on DTI in the MSC-treated group was greater than in the vehicle group.
- The degree of interhemispheric cortical connections labeled with AAV tracing techniques was greater in the MSC-treated group than the vehicle group.
- The preservation/restoration of anatomical connections between the hemispheres may contribute to functional improvements from cell-based therapy with MSCs for stroke.

1. Introduction:

Stroke affecting the motor cortex induces interhemispheric network disturbances and disrupts the white matter fibers through the corpus callosum connecting the bilateral motor cortex with motor performance deficits (Li et al., 2015). The restored interhemispheric bilateral motor cortex connectivity may play a beneficial role to exert endogenous functional recovery after stroke (Liu et al., 2015).

Intravenous infusion of mesenchymal stem cells (MSCs) after cerebral stroke improves functional outcome in experimental stroke models (Chen et al., 2016; Honmou et al., 2011; Moisan et al., 2016; Nakamura et al., 2017; Nakazaki et al., 2017; Sasaki et al., 2016; Suzuki et al., 2013; Vahidy et al., 2016). Suggested therapeutic mechanisms of MSCs include secretion of neurotrophic factors that can provide for neuroprotection, axonal regeneration, remyelination, and synaptogenesis (Ding et al., 2013; Honmou et al., 2012; Kocsis and Honmou, 2012; Liu et al., 2009; Sasaki et al., 2016; Ye et al., 2013)

In this study, we used both diffusion tensor imaging (DTI) and GFP-expressing adeno-associated virus (AAV)-mediated neuroanatomical tracing to detect anatomical restoration of cortical interhemispheric connections through corpus callosum after intravenous infusion of MSCs in a rat middle cerebral artery occlusion (MCAO) model. We also performed quantitative analysis of thickness of corpus callosum and synaptic puncta in the contra-infarcted motor cortex connected to the corpus callosum.

2. Results

2.1 Ischemic lesion volume by magnetic resonance image analysis

The ischemic lesion volume was estimated for the experimental groups using *in vivo* MRI

(see Method section). T2-weighted images (T2WI) were obtained from the groups at pre MCAO, day 1, day 4, day 7, day 14, day 28, and day 42 after MCAO induction (Fig. 1A). These coronal forebrain sections were obtained at the level of the caudate-putamen complex. Diffusion weighted imaging (DWI) also were obtained 6 h after MCAO and confirmed no difference in the initial stroke volume between the groups (MSC group = 285.65 ± 10.01 mm^3, vehicle group = 276.78 ± 9.95 mm^3; $p = 0.62$).

The lesion volume (mm^3) was determined by analyzing T2WI high-intensity areas on serial images collected through the cerebrum (see Methods). The MSC-treated group displayed a significantly greater volume reduction compared with the vehicle group rats at day 7 (MSC group = 245.47 ± 7.25 mm^3, vehicle group = 292.40 ± 14.04 mm^3; $p < 0.05$), day 14 (MSC group = 222.02 ± 7.24 mm^3, vehicle group = 274.55 ± 15.01 mm^3; $p < 0.05$), day 28 (MSC group = 199.02 ± 6.85 mm^3, vehicle group = 244.05 ± 8.00 mm^3; $p < 0.01$), and day 42 (MSC group = 176.91 ± 5.81 mm^3, vehicle group = 227.72 ± 6.08 mm^3; $p < 0.005$) (Fig. 1B).

2.2 Behavioral function

The maximum velocity at which the rats could run on a motor-driven treadmill was recorded. Before MCAO all rats reached a velocity of 70 m/min. Twenty-four hours after MCAO maximum velocity on the treadmill test was at its maximum deficit. The MSC-infused groups had significantly greater maximum velocity at day 7 (MSC group = 37.77 ± 4.52 m/min, vehicle group = 19.44 ± 3.42 m/min; $p < 0.05$), day 14 (MSC group = 49.55 ± 5.35 m/min, vehicle group = 26.66 ± 3.23 m/min; $p < 0.01$), day 28 (MSC group = 60.22 ± 3.72 m/min, vehicle group = 38.88 ± 2.67 m/min; $p < 0.01$), and day 42 (MSC

group = 66.22 ± 1.49 m/min, vehicle group = 37.66 ± 3.23 m/min; $p < 0.01$) than the vehicle group. These results indicate that intravenous administration of MSCs improved functional outcome. These data are summarized in Fig. 2.

Taken together with the analysis of ischemic volume evaluated with MRI T2WI, the results from the model system used in this study were consistent with previous studies, where the intravenous infusion of MSCs provided functional improvements and enhanced reduction of the ischemic lesion volume.

2.3 DTI analysis

DTI tractography demonstrated that more preserved interhemispheric cortical connections from the motor cortex in the ischemic hemisphere through corpus callosum was observed in the MSC-treated animals (Fig. 3D) compared to the vehicle group (Fig. 3C) following MCAO. Quantitative analysis revealed that the number of "tracks" in the MSC group (217.25 ± 92.45) was 7 times greater than the vehicle group (30.50 ± 8.00; $p < 0.05$).

2.4 Analysis of GFP-expressing AAV-based tracing

We used a GFP-expressing AAV vector to trace interhemispheric cortical connections through corpus callosum following intravenous infusion of MSCs or vehicle in MCAO. We injected the viruses in the motor cortex in the ischemic hemisphere to transduce layer V pyramidal axons as previously described (Soderblom et al., 2015). Although the GFP signal intensity from the AAV vector at the injection site in the ischemic hemisphere was similar in both groups (Fig. 4A, 4E), the intensity in axons of the corpus callosum and the

contralateral cortex was significantly greater in the MSC group (Fig. 4E-4H) than the vehicle group (Fig. 4A-4D). Confocal microscopic observation revealed that the number of transduced GFP^+ cells located in layer V in the MSC group (Fig.4F, 4H) was greater than in the vehicle group (Fig. 4B, 4D) and the intensity of transduced GFP^+ apical dendrites in layer II/III , which are elaborated for layer V neurons, was likewise greater in the MSC group (Fig. 4G) than the vehicle group (Fig. 4C). Quantitative analysis of dendrites in layer II/III, and cell bodies in layer V are shown in Fig. 5A and Fig. 5B, respectively. These histological results were consistent with the results of DTI showing preserved interhemispheric cortical connections through corpus callosum following intravenous infusion of MSCs in MCAO.

2.5 Expression of synaptophysin

To determine whether there were synaptic changes in the projection neurons in the area of cortex contralateral to the lesion site, synaptic density in the motor cortex in the contralateral hemisphere was examined at day 42 after stroke induction. Confocal microscopic imaging demonstrated that numerous synaptic puncta were present on AAV-transduced GFP^+ neurons and dendrites in the contralateral cortex (Fig. 6B).

Synaptophysin$^+$ puncta were quantified to determine synaptic density (Fig. 6C-6G). The density of synaptic puncta in layer II/III (Fig. 6D) and layer V (Fig. 6G) in the MSC-treated group in the motor cortex of the contralateral hemisphere was higher than in both layer II/III (Fig. 6C) and layer V (Fig. 6F) of the vehicle groups. These results are summarized in Fig. 6E, 6H, respectively. These data suggest preserved synaptic plasticity

of interhemispheric cortical connections through corpus callosum following intravenous infusion of MSCs in stroke.

2.6 Thickness of corpus callosum

Quantification of the thickness of the corpus callosum was examined (Fig. 7). Corpus callosum thickness evaluated with Nissl staining was greater in the MSC group (Fig. 7B, Fig. 7C: 344.90 ± 3.66 μm) than the vehicle group (Fig. 7A, Fig. 7C: 277.48 ± 7.44 μm) (p <0.05). This result was confirmed with T2WI (Fig. 7D; MSC: 349.50 ± 9.49 μm, vehicle: 262.25 ± 24.46 μm, p<0.05). These data indicate that MSC delivery preserves corpus callosum thickness.

3. Discussion

In this study, we demonstrated preserved interhemispheric cortical connections through corpus callosum utilizing both DTI tractography and viral vector-based neuroanatomical tracing methods with a GFP-expression AAV. We also found that both thickness of corpus callosum and the expression of synaptophysin observed in the ipsilateral neurons projecting to contralateral cortex were preserved following intravenous infusion of MSCs after cerebral ischemia using our consistent and reliable stroke model with cellular therapy system.

Cell-based therapeutic approaches with MSCs are being considered for a number of neurological diseases including stroke (Honmou et al., 2012; Morita et al., 2016; Nakamura et al., 2017; Sasaki et al., 2011; Sasaki et al., 2016). Suggested therapeutic mechanisms include neuroprotection, remodeling of neural circuits, restoration of blood

brain barrier, reduction of inflammatory infiltration and demyelination, and elevation of trophic factors that may be neuroprotective and promote synaptogenesis (Sasaki et al., 2009b; Sasaki et al., 2016). In addition to these suggested mechanisms, preserved interhemispheric cortical connections after stroke as shown in this study could be considered as another mechanism.

First, we have shown that a greater number of neural fibers detected with DTI tractography was observed in the MSC treated animals compared to the vehicle group. Thus, we hypothesized preservation of interhemispheric cortical connections through the corpus callosum projecting from the infarcted cortex through the corpus callosum (Suzuki et al., 2013). Transcallosal axonal sprouting after cortical infarction has been reported (Carmichael and Chesselet, 2002). It is, however, conceivable that sprouting of axons from the infarcted cortex into the contra-infarct cortex could contribute to the transcallosal projectons and increased functional activity (Suzuki et al., 2013).

Second, we have demonstrated in this study that infusion of MSCs led to a greater number of neural fibers, in accordance with the DTI tractography. Using a combination of retrograde lentiviral vectors and AAV injected to opposite sides of motor cortex for double infection of intact mice, Watakabe et al. (2014) elegantly showed that axonal projections of callosally-projecting corticocortical neurons in motor cortex have complex axonal collateral branches (Watakabe et al., 2014). Consistent with this previous work (Watakabe et al., 2014), interhemispheric cortical axonal projections through corpus callosum were observed by labeling with a GFP-expressing AAV in our study. There was a more intense trajectory of callosal corticocortical axonal sprouting in MSC-treated animals than in the vehicle group in our study. The intensity of apical

dendrites of transduced GFP^+ neurons in layer II/III, which originate from layer V, was greater in the MSC group than the vehicle group. The number of transduced GFP^+ cells in the layer V was accordingly greater in the MSC group than in the vehicle group. Taken together, our data demonstrated preserved neural fibers following infusion of MSCs as calculated by DTI tractography and histologically verified utilizing an AAV-based neuroanatomical tracer technique.

Finally, we evaluated whether preserved synapses can be observed in the axonal projections to the contra-infarct cortex through the corpus callosum after intravenous infusion of MSCs. This would build on studies attributing recovery to axonal sprouting and synaptogenesis, perhaps in response to neurotrophic factors derived from infused MSCs (Ren et al., 2012). Here, we observed that intravenous infusion of MSCs significantly preserved the expression of synaptophysin in the contra-infarcted hemisphere suggesting the protection and/or regeneration of synaptic puncta in callosal projections in cortical areas contralateral to the infarcted cortex. The greater thickness of the corpus callosum may likewise be attributable to preservation of transcallosal projections between the hemispheres. Either process might contribute to functional improvement from cerebral infarction. Although it is difficult to distinguish between preserved or sprouting/synaptogenesis in the present study, it is conceivable that the expression of synaptophysin which we observed might include newly formed synaptic formation as well.

4. Conclusion

In summary, we have shown distinct preservation of interhemispheric cortical connections through corpus callosum following intravenous infusion of MSCs in a rat model of cerebral infarction utilizing DTI tractography and AAV neuroanatomical tracing techniques. This anatomical preservation of the motor cortex in the contra-infarcted hemisphere may contribute to functional improvements following MSC therapy for cerebral stroke.

5. Experimental Procedures:

5.1 Ethics statement

The Animal care and use committee of Sapporo Medical University approved the use of animals in this study; all procedures were carried out in accordance with institutional guidelines.

5.2 Preparation of mesenchymal stem cells from rat bone marrow

The methodology of preparing an MSC culture was based upon our previous studies (Morita et al., 2016; Nakamura et al., 2017; Sasaki et al., 2016). In brief, bone marrow was obtained from the femoral bones of adult rats. The marrow was then diluted to 20 ml with Dulbecco's modified Eagle's medium (DMEM) (SIGMA, St. Louis, MO, USA) and supplemented with 10% heat-inactivated fetal bovine serum (FBS) (Thermo Fisher Scientific Inc., Waltham, MA, USA), 2 mM l-glutamine (SIGMA), 100 U/ml penicillin, 0.1 mg/ml streptomycin (Thermo Fisher Scientific Inc.) and incubated for 3 days (5% CO_2, 37°C). When cultures almost reached confluence, the adherent cells were detached

with trypsin-EDTA solution (SIGMA) and subcultured at 1×10^4 cells/ml. In the present study, we used MSCs after exactly three passages.

5.3 Cerebral ischemic model

We induced transient MCAO for 90 min by using a previously described method of intraluminal vascular occlusion (Honma et al., 2006; Iihoshi et al., 2004; Nakazaki et al., 2017; Sasaki et al., 2009a). Adult male SD (280–320 g) rats were anesthetized with an intraperitoneal (i.p) injection of ketamine (75 mg/kg) and xylazine (10 mg/kg). A length of 20.0–22.0 mm 3–0 surgical MONOSOF suture with the tip rounded by heating near a flame was advanced from the external carotid artery into the lumen of the internal carotid artery until it blocked the origin of the middle cerebral artery. Ninety minutes after MCAO induction, reperfusion was performed by withdrawal of the suture until the tip cleared the internal carotid artery. Physiological parameters (rectal temperature, blood pH, pO2, pCO2, blood pressure) were maintained within normal ranges during surgery and transplantation procedures for all animals and did not statistically differ between the groups (Honma et al., 2006; Iihoshi et al., 2004; Sasaki et al., 2009a).

5.4 Mesenchymal stem cell infusion procedures

Transplantation protocols consisted of two groups. In the MSC-treated group (n=12), rats were injected intravenously with MSCs (1.0×10^6 cells each) in 1 ml total fluid volume (fresh DMEM), through the femoral vein 2 hours after the MCAO (and just after the initial DWI). In the vehicle group (n=12), rats were injected intravenously with medium alone (fresh DMEM only) through the femoral vein (without donor cell administration) 2 hours after MCAO (just after the initial DWI-MRI). We confirmed higher cell viability

(>99%) with 0.4% trypan blue immediately after the procedure. All rats, including rats in the vehicle group, were injected daily with cyclosporine A (10 mg/kg, i.p.) (Nakamura et al., 2017; Sasaki et al., 2016).

5.5 Treadmill stress test

Rats were trained 20 min/day for 2 days a week to run on a motor-driven treadmill (Muromachi Inc, Tokyo, Japan) at a speed of 20 m/min with a slope of 20° before MCAO. The maximum speed at which the rats could run on a motor-driven treadmill was recorded at day 1, 4, 7, 14, 28, and 42 after MCAO (n=12/group).

5.6 MRI

All MRI measurements were performed using a 7-Tesla, 18 cm bore superconducting magnet (Oxford Magnet Technologies) interfaced to a UNITY INOVA console (Oxford Instruments, UK, and Varian Inc., Palo Alto, CA). A 38 mm diameter birdcage coil was used as the radio frequency signal transmitter and receiver.

For *in vivo* imaging (n=12/group), DWI were obtained within 2 hours after MCAO induction using a spin-echo pulse sequence to acquire 1.0-mm-thick coronal sections with a 0.5 mm gap using a b-value = 1000 s/mm^2, acquisition matrix = 128 × 128, FOV = 30 mm × 30 mm, TR/TE = 3000/37 mm^2. We included the animals for standardization with strict criteria (the initial stroke volume by DWI was within 240–360 mm^3). T2WIs were obtained at pre-MCAO, and day 1, day 4, day 7, day 14, day 28, and day 42 after MCAO using a spin-echo pulse sequence to acquire 1.0-mm-thick coronal

sections with a 0.5 mm gap using an acquisition matrix = 256 × 128, FOV = 30 mm × 30 mm, and TR/TE = 3000/30 ms.

The ischemic lesion area was calculated from T2WIs using imaging software (Scion Image, Version Beta 4.0.2, Scion Corporation), based on a previously described method (Nakamura et al., 2017; Sasaki et al., 2016; Suzuki et al., 2013). Briefly, after optimal adjustment of contrast, the edges of the lesions, defined as where the signal intensity was 1.25 times higher than the counterpart in the contralateral brain lesion, were manually traced on each of the nine coronal slices, which completely covered the middle cerebral artery territory in all animals. The hyperintensive areas were then summed and multiplied by the slice thickness plus interslice gap to calculate lesion volumes. It should be noted that although the high intensity area on T2WI just after MCAO induction was not clear enough to measure stroke volume, the high intensity area on DWI at this time (within 2 hours after MCAO induction) point could be used to evaluate the initial stroke volume after MCAO induction.

Corpus callosum (CC) thickness was measured with T2WIs (n=12 per group) using NIH ImageJ software (version 1.45s, National Institutes of Health, USA) at the midline on bregma –0.26 mm level slices (modified from Paxinos and Watson (Paxinos and Watson, 2007).

For *ex vivo* DTI imaging (n=4/group), at day 42, rats were deeply anesthetized with ketamine and xylazine (75/10 mg/kg, intraperitoneally) and transcardially perfused with cold PBS followed by a 4% paraformaldehyde/balance PBS solution. The cranium was removed, and the brain was stored in PBS containing 4% paraformaldehyde for 2 weeks. Before ex vivo imaging, the chemically fixed brain was trimmed to fit into an

acrylic tube filled with fluorinert (Sumitomo 3M Limited, Tokyo, Japan) that minimizes susceptibility artifacts at the interface (Kelley et al., 2014).

DTI was obtained using a spin-echo pulse sequence. A diffusion sensitized preparation was performed using Stejskal-Tannar encoding scheme. Forty-four contiguous 350 μm coronal sections were acquired using b-value = 809 s/mm^2 (δ = 8.5 ms, Δ = 12.5 ms, gradient amplitude = 90 mT/m), acquisition matrix = 128 × 128 (reconstructed using a 128 × 128 image matrix), FOV = 25.6 mm × 25.6 mm, TR/TE = 5000/30 ms, number of signal average = 10. One b0 image and six high b-value images were acquired with diffusion sensitization along each of six non-collinear diffusion gradient vectors: [0, 1, 1], [0, 1, -1], [1, 0, 1], [-1, 0, 1], [1, 1, 0], and [1, -1, 0]. Total imaging time was approximately 13 h. DTI data were processed with Diffusion Toolkit, and Trackvis software (http://trackvis.org) (Wedeen et al., 2008). To estimate diffusion tensors, the Interpolated Streamline propagation algorithm was applied for deterministic tractography with a fractional anisotropy (FA) threshold of 0.15 and an angle threshold of 20°. We manually placed the seeding region-of-interest (ROI) for fiber tracking within the bilateral anterior cerebral cortex, which organizes interhemispheric connections through the corpus callosum. The ROI was set on the basis of two-dimensional T2WIs and a color-coded fractional anisotropy map in each coronal slice. Consequently, three-dimensional ROIs were defined as the ipsi- and contralateral anterior cortex, respectively. The ROI locations were determined using histology atlas (Paxinos and Watson, 2007), and a DTI atlas (Papp et al., 2014). Tracking of fibers that were connecting bilateral ROIs was performed. The corticocortical connection was defined by the number of “tracks” of fibers passing through bilateral ROIs, simultaneously.

5.7 GFP-expressing AAV tracer injections

GFP-encoding AAVs with a CAG promoter (GFP-CAG-AAV; serotype 8) were purchased from Vector Biolabs (Philadelphia, PA). At day 42 after MCAO, rats were placed on a stereotaxic frame under the anesthesia induced by intraperitoneal injection of ketamine (75 mg/kg) and xylazine (10 mg/kg). To label cortical fibers projecting to contralateral cerebral cortex from survived neurons located around the ischemic lesion, a craniotomy was performed to expose the right sensorimotor cortex. The AAVs were injected into the ischemic cortex using a nanoliter-injector (World Precision Instrument Inc., Sarasota, FL) attached to a pulled glass pipette. Six injections (AAVs; 4.0×10^{10} genome copy /μl, 0.5 μl per site) were performed at the following coordinates: 1.25 mm lateral; 1.0 mm, 0.5 mm depth, and 0.2 mm, 0.6 mm, 1.0 mm posterior to bregma. The needle was left in place for 3 min before moving to the next site. The sections were examined using a confocal microscopy (excitation/emission = 405/488: Zeiss LSM780 ELYRA S.1 system). Sections were viewed directly for GFP fluorescence.

5.8 Immunohistochemistry

Rats were perfused transcardially with cold phosphate-buffered saline (PBS) followed by 4% paraformaldehyde under deep anesthesia with an intraperitoneal injection of ketamine (75 mg/kg) and xylazine (10 mg/kg). Whole brains were dissected out, post-fixed in 4% paraformaldehyde overnight, and cryoprotected in 30% sucrose/phosphate-buffered saline at 4°C. Samples were stored at 80°C until use. Coronal sections were cut to 50 μm thickness using a cryostat (Sakura Seiki Co, Tokyo, Japan). One section per animal was

selected according to the rat stereotaxic atlas (bregma -0.4 mm) (Paxinos and Watson, 2007), washed in PBS-0.1% Tween 20 (PBS-T) 3 times, blocked in 5% normal goat serum/0.3 % Triton X-100 in PBS at room temperature for 30 min, and incubated in primary antibodies diluted in 5% normal goat serum/0.3% Triton X-100 /PBS at 4°C overnight.

We used rabbit anti-synaptophysin antibody (1:500; Novus/ NB110-57606) as a presynaptic marker (synaptophysin is a presynaptic vesicle protein and indicator of presynaptic plasticity and synaptogenesis), and chicken anti-GFP antibody (1:1,000; Abcam, ab13970) for detection of GFP. After washing in PBS-T 4 times, sections were incubated in secondary antibodies, which were AF488-conjugated goat anti-rabbit immunoglobulin G (1:1,000; Jackson/711-165-152) for synaptophysin and AF 488-conjugated goat anti-chicken immunoglobulin Y (1:1,000; Abcam, 150173) for GFP, counter-stained with 4',6-diamidino-2-phenylindole (DAPI), and coverslipped with Vectashield (Vector Laboratories, Burlingame, California).

5.9 Quantitative analysis of GFP- expressing AAV

AAV-transduced GFP^+ cells of layer II/III and layer V in the contralateral motor cortex in the ischemic lesion side projecting through the corpus callosum were quantified using a light microscope (BX51, Olympus) equipped with an automatic stage and coupled to a computer running Stereo Investigator software (MicroBrightField, Colchester, VT, USA). Four rats in each group were used. One in every 10 serial sections (50 μm thick) for cerebral mortar cortex were selected for analysis. Contours were drawn around for layer II/III and layer V in the contralateral cerebral cortex, and cell counting was performed.

To estimate the number of GFP^+ cell, the optical fractionator method was used to count the cells in a 3-dimentional counting in a frame of 150 × 100 × 40 μm using a sampling grid of 1000 × 1000 μm for GFP^+ cells in the layer II/III and layer V of contralateral motor cortex. The average Schaffer coefficient of error for cell counting was 0.04-0.09.

5.10 Quantitative analysis of synaptic change

The sections were examined by confocal microscopy (excitation/emission = 405/561; LSM780 ELYRA S.1 system). For quantitative analysis of synaptophysin, confocal images were collected from layer the II/III and the layer V in the motor cortex in the contralateral hemisphere according to the rat stereotaxic atlas (bregma -0.4 mm) (Paxinos and Watson, 2007). ROIs of 2,048 × 2,048 pixels were placed to quantify the expression of synaptophysin. The coordinate relative to the bregma for the center of the ROI was at -0.40 mm caudal, 2 mm lateral, 0.5 mm depth to target layer II and 1.5 mm depth to target layer V (Sasaki et al., 2016). Gain thresholds and amplitude offsets were kept constant for each section. Averaged synaptic puncta per field were counted using the ImageJ Software in each scanned field (4 fields per layer per animal) from vehicle group (n=4), and MSC group (n=4).

5.11 Thickness of corpus callosum

Corpus callosum thickness was measured with Nissl staining using NIH ImageJ at the midline on bregma –0.26 mm level slices, the same location of MRI analysis. Four rats in each group were used.

5.12 Statistical analysis

All statistical analyses were performed using SPSS 20 for Macintosh (SPSS, Inc, IL, USA). Comparison of the two groups was performed using Mann-Whitney *U* tests. Error bars represent mean ± SEM.

Disclosure:

None.

Acknowledgments

This work was supported in part by JSPS KAKENHI grant Numbers 15K10365, 16K10730, 17K10901, 17K01513, the AMED Translational Research Network Program (JP16lm0103003) and the RR&D Service of Department of Veterans Affairs (B7335R, B9260L), the NMSS [RG2135], CT Stem Cell Research Program (12-SCB-Yale-05).

Figure legends

Figure 1.

Estimation of the ischemic lesion volume for the vehicle and the MSC-treated groups. The T2WIs at pre MCAO, day 1, day 4, day 7, day 14, day 28 and day 42, after MCAO induction (A). The lesion volume measured from high-intensity areas on T2WI at pre MCAO, day 1, day 4, day 7, day 14, day 28, and day 42 after MCAO induction (B). Scale bar = 5mm. * $p < 0.05$, ** $p < 0.01$.

Figure 2.

The maximum velocity at which the rats could run on a motor-driven treadmill was recorded at day 1, 4, 7, 14, 28, and 42 after MCAO. * $p < 0.05$, ** $p < 0.01$.

Figure 3.

Evaluation of interhemispheric cortical connections from the motor cortex in the ischemic hemisphere through corpus callosum. DTI tractography depicted that interhemispheric cortical connections from the motor cortex in the ischemic hemisphere through corpus callosum in the vehicle (A) and in the MSC treated group (B). The number of "tracks" on DTI tractography (C). * $p < 0.05$.

Figure 4.

Tracing if the interhemispheric cortical connections through corpus callosum using a GFP-expressing AAV vector. AAV injected in the ischemic motor cortex was observed in the contralateral cortex. The signal intensity in the contralateral cortex in the MSC-

treated group (E) was significantly greater than in the vehicle group (A). Confocal observation of the contralateral cortex in the vehicle group (B) and MSC treated group (F). The number of transduced GFP^+ cells located in layer II/III and V in the MSC treated group (G, H) was greater than that in the vehicle group (C, D). Scale bars = 750 μm (E), 300 μm (F), 30 μm (G, H).

Figure 5.

Quantification of the number of transduced GFP^+ cells in the layer II/III (A) and the layer V (B) in the vehicle and the MSC treated group, respectively. * $p < 0.05$.

Figure 6.

Examination of the synaptic density in the motor cortex in the contralateral hemisphere at day 42 after MCAO induction. Location of the confocal microscopic images (A). Confocal microscopic image demonstrated that numerous synaptic puncta (red) are observed around the AAV transduced GFP^+ neurons (green) and dendrites (green) (B). Representative images from immunohistochemical analysis of synaptophysin layer II/III (C, D) and layer V (F, G) in the vehicle and the MSC-treated group, respectively. Quantification of the density of synaptic puncta in the layer II/III (E) and the layer V (H). Scale bars = 10 μm (B), 5 μm (G). * $p < 0.05$.

Figure 7.

Quantification of the thickness of the corpus callosum. The thickness was measured from Nissl staining images for the corpus callosum (arrow-head) in the vehicle and the MSC-

treated group (A, B). The thickness of the corpus callosum measured from Nissl staining images (C). The thickness of the corpus callosum measured from T2WI (D). Scale bar = 20 μm. * $p < 0.05$.

References:

Carmichael, S.T., Chesselet, M.F., 2002. Synchronous neuronal activity is a signal for axonal sprouting after cortical lesions in the adult. J Neurosci. 22**,** 6062-70.

Chen, K.H., Chen, C.H., Wallace, C.G., Yuen, C.M., Kao, G.S., Chen, Y.L., Shao, P.L., Chen, Y.L., Chai, H.T., Lin, K.C., Liu, C.F., Chang, H.W., Lee, M.S., Yip, H.K., 2016. Intravenous administration of xenogenic adipose-derived mesenchymal stem cells (ADMSC) and ADMSC-derived exosomes markedly reduced brain infarct volume and preserved neurological function in rat after acute ischemic stroke. Oncotarget. 7**,** 74537-74556.

Ding, X., Li, Y., Liu, Z., Zhang, J., Cui, Y., Chen, X., Chopp, M., 2013. The sonic hedgehog pathway mediates brain plasticity and subsequent functional recovery after bone marrow stromal cell treatment of stroke in mice. J Cereb Blood Flow Metab. 33**,** 1015-24.

Honma, T., Honmou, O., Iihoshi, S., Harada, K., Houkin, K., Hamada, H., Kocsis, J.D., 2006. Intravenous infusion of immortalized human mesenchymal stem cells protects against injury in a cerebral ischemia model in adult rat. Exp Neurol. 199**,** 56-66.

Honmou, O., Houkin, K., Matsunaga, T., Niitsu, Y., Ishiai, S., Onodera, R., Waxman, S.G., Kocsis, J.D., 2011. Intravenous administration of auto serum-expanded autologous mesenchymal stem cells in stroke. Brain. 134**,** 1790-807.

Honmou, O., Onodera, R., Sasaki, M., Waxman, S.G., Kocsis, J.D., 2012. Mesenchymal stem cells: therapeutic outlook for stroke. Trends Mol Med. 18**,** 292-7.

Iihoshi, S., Honmou, O., Houkin, K., Hashi, K., Kocsis, J.D., 2004. A therapeutic window for intravenous administration of autologous bone marrow after cerebral ischemia in adult rats. Brain Res. 1007**,** 1-9.

Kelley, B.J., Harel, N.Y., Kim, C.Y., Papademetris, X., Coman, D., Wang, X., Hasan, O., Kaufman, A., Globinsky, R., Staib, L.H., Cafferty, W.B., Hyder, F., Strittmatter, S.M., 2014. Diffusion tensor imaging as a predictor of locomotor function after experimental spinal cord injury and recovery. J Neurotrauma. 31**,** 1362-73.

Kocsis, J.D., Honmou, O., 2012. Bone marrow stem cells in experimental stroke. Prog Brain Res. 201**,** 79-98.

Li, Y., Wu, P., Liang, F., Huang, W., 2015. The microstructural status of the corpus callosum is associated with the degree of motor function and neurological deficit in stroke patients. PLoS One. 10**,** e0122615.

Liu, J., Qin, W., Zhang, J., Zhang, X., Yu, C., 2015. Enhanced interhemispheric functional connectivity compensates for anatomical connection damages in subcortical stroke. Stroke. 46**,** 1045-51.

Liu, Z., Zhang, R.L., Li, Y., Cui, Y., Chopp, M., 2009. Remodeling of the corticospinal innervation and spontaneous behavioral recovery after ischemic stroke in adult mice. Stroke. 40**,** 2546-51.

Moisan, A., Favre, I., Rome, C., De Fraipont, F., Grillon, E., Coquery, N., Mathieu, H., Mayan, V., Naegele, B., Hommel, M., Richard, M.J., Barbier, E.L., Remy, C., Detante, O., 2016. Intravenous Injection of Clinical Grade Human MSCs After Experimental Stroke: Functional Benefit and Microvascular Effect. Cell Transplant. 25**,** 2157-2171.

Morita, T., Sasaki, M., Kataoka-Sasaki, Y., Nakazaki, M., Nagahama, H., Oka, S., Oshigiri, T., Takebayashi, T., Yamashita, T., Kocsis, J.D., Honmou, O., 2016. Intravenous infusion of mesenchymal stem cells promotes functional recovery in a model of chronic spinal cord injury. Neuroscience. 335**,** 221-31.

Nakamura, H., Sasaki, Y., Sasaki, M., Kataoka-Sasaki, Y., Oka, S., Nakazaki, M., Namioka, T., Namioka, A., Onodera, R., Suzuki, J., Nagahama, H., Mikami, T., Wanibuchi, M., Kocsis, J.D., Honmou, O., 2017. Elevated brain derived neurotrophic factor (BDNF) levels in plasma but not serum reflect in vivo functional viability of infused mesenchymal stem cells after middle cerebral artery occlusion in rat. J Neurosurg Sci.

Nakazaki, M., Sasaki, M., Kataoka-Sasaki, Y., Oka, S., Namioka, T., Namioka, A., Onodera, R., Suzuki, J., Sasaki, Y., Nagahama, H., Mikami, T., Wanibuchi, M., Kocsis, J.D., Honmou, O., 2017. Intravenous infusion of mesenchymal stem cells inhibits intracranial hemorrhage after recombinant tissue plasminogen activator therapy for transient middle cerebral artery occlusion in rats. J Neurosurg. 127**,** 917-926.

Papp, E.A., Leergaard, T.B., Calabrese, E., Johnson, G.A., Bjaalie, J.G., 2014. Waxholm Space atlas of the Sprague Dawley rat brain. Neuroimage. 97**,** 374-86.

Paxinos, G., Watson, C., 2007. The Rat Brain in Stereotaxic Coordinates. In 123Library. Vol., ed.^eds. Academic Press.

Ren, G., Chen, X., Dong, F., Li, W., Ren, X., Zhang, Y., Shi, Y., 2012. Concise review: mesenchymal stem cells and translational medicine: emerging issues. Stem Cells Transl Med. 1**,** 51-8.

Sasaki, M., Honmou, O., Kocsis, J., 2009a. A rat middle cerebral artery occlusion model and intravenous cellular delivery. Methods Mol Biol. 549**,** 187-95.

Sasaki, M., Radtke, C., Tan, A.M., Zhao, P., Hamada, H., Houkin, K., Honmou, O., Kocsis, J.D., 2009b. BDNF-hypersecreting human mesenchymal stem cells promote functional recovery, axonal sprouting, and protection of corticospinal neurons after spinal cord injury. J Neurosci. 29**,** 14932-41.

Sasaki, M., Honmou, O., Radtke, C., Kocsis, J.D., 2011. Development of a middle cerebral artery occlusion model in the nonhuman primate and a safety study of i.v. infusion of human mesenchymal stem cells. PLoS One. 6**,** e26577.

Sasaki, Y., Sasaki, M., Kataoka-Sasaki, Y., Nakazaki, M., Nagahama, H., Suzuki, J., Tateyama, D., Oka, S., Namioka, T., Namioka, A., Onodera, R., Mikami, T., Wanibuchi, M., Kakizawa, M., Ishiai, S., Kocsis, J.D., Honmou, O., 2016. Synergic Effects of Rehabilitation and Intravenous Infusion of Mesenchymal Stem Cells After Stroke in Rats. Phys Ther. 96**,** 1791-1798.

Soderblom, C., Lee, D.H., Dawood, A., Carballosa, M., Jimena Santamaria, A., Benavides, F.D., Jergova, S., Grumbles, R.M., Thomas, C.K., Park, K.K., Guest, J.D., Lemmon, V.P., Lee, J.K., Tsoulfas, P., 2015. 3D Imaging of Axons in Transparent Spinal Cords from Rodents and Nonhuman Primates. eNeuro. 2.

Suzuki, J., Sasaki, M., Harada, K., Bando, M., Kataoka, Y., Onodera, R., Mikami, T., Wanibuchi, M., Mikuni, N., Kocsis, J.D., Honmou, O., 2013. Bilateral cortical hyperactivity detected by fMRI associates with improved motor function following intravenous infusion of mesenchymal stem cells in a rat stroke model. Brain Res. 1497**,** 15-22.

Vahidy, F.S., Rahbar, M.H., Zhu, H., Rowan, P.J., Bambhroliya, A.B., Savitz, S.I., 2016. Systematic Review and Meta-Analysis of Bone Marrow-Derived Mononuclear Cells in Animal Models of Ischemic Stroke. Stroke. 47**,** 1632-9.

Watakabe, A., Takaji, M., Kato, S., Kobayashi, K., Mizukami, H., Ozawa, K., Ohsawa, S., Matsui, R., Watanabe, D., Yamamori, T., 2014. Simultaneous visualization of extrinsic and intrinsic axon collaterals in Golgi-like detail for mouse corticothalamic and corticocortical cells: a double viral infection method. Front Neural Circuits. 8**,** 110.

Wedeen, V.J., Wang, R.P., Schmahmann, J.D., Benner, T., Tseng, W.Y., Dai, G., Pandya, D.N., Hagmann, P., D'Arceuil, H., de Crespigny, A.J., 2008. Diffusion spectrum magnetic resonance imaging (DSI) tractography of crossing fibers. Neuroimage. 41**,** 1267-77.

Ye, X., Yan, T., Chopp, M., Zacharek, A., Ning, R., Venkat, P., Roberts, C., Chen, J., 2013. Combination BMSC and Niaspan treatment of stroke enhances white matter remodeling and synaptic protein expression in diabetic rats. Int J Mol Sci. 14**,** 22221-32.

Figure1

Click here to download high resolution image

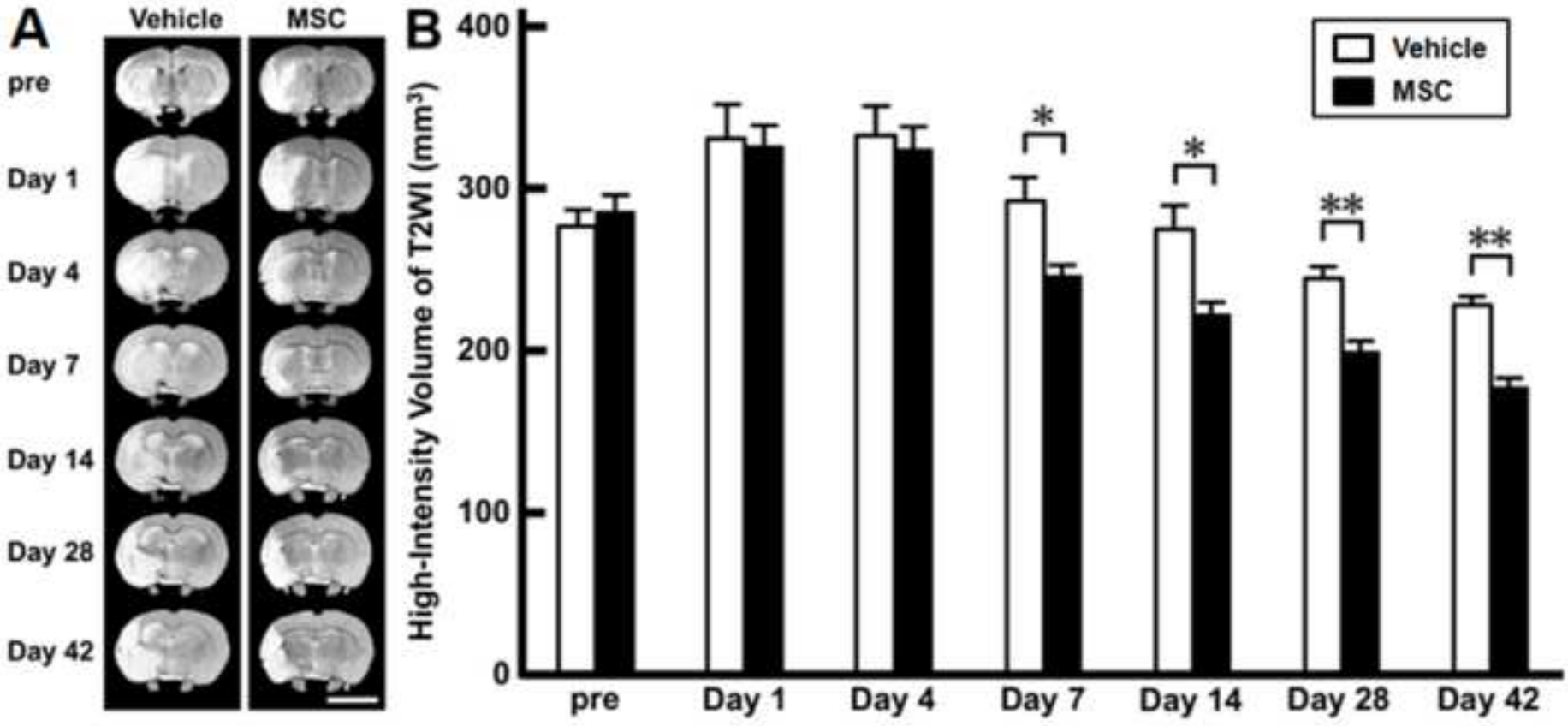

Figure2
Click here to download high resolution image

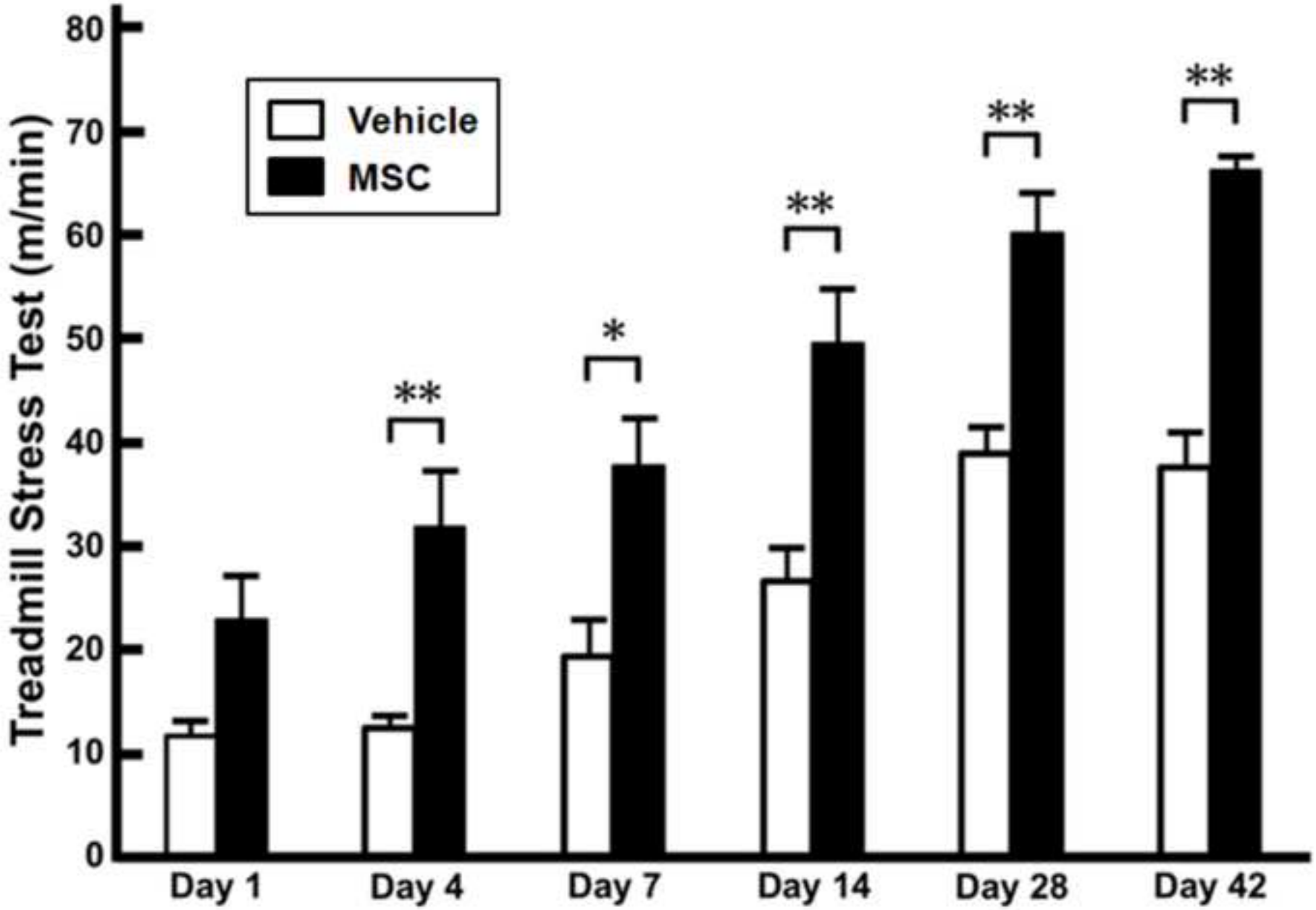

Figure3
Click here to download high resolution image

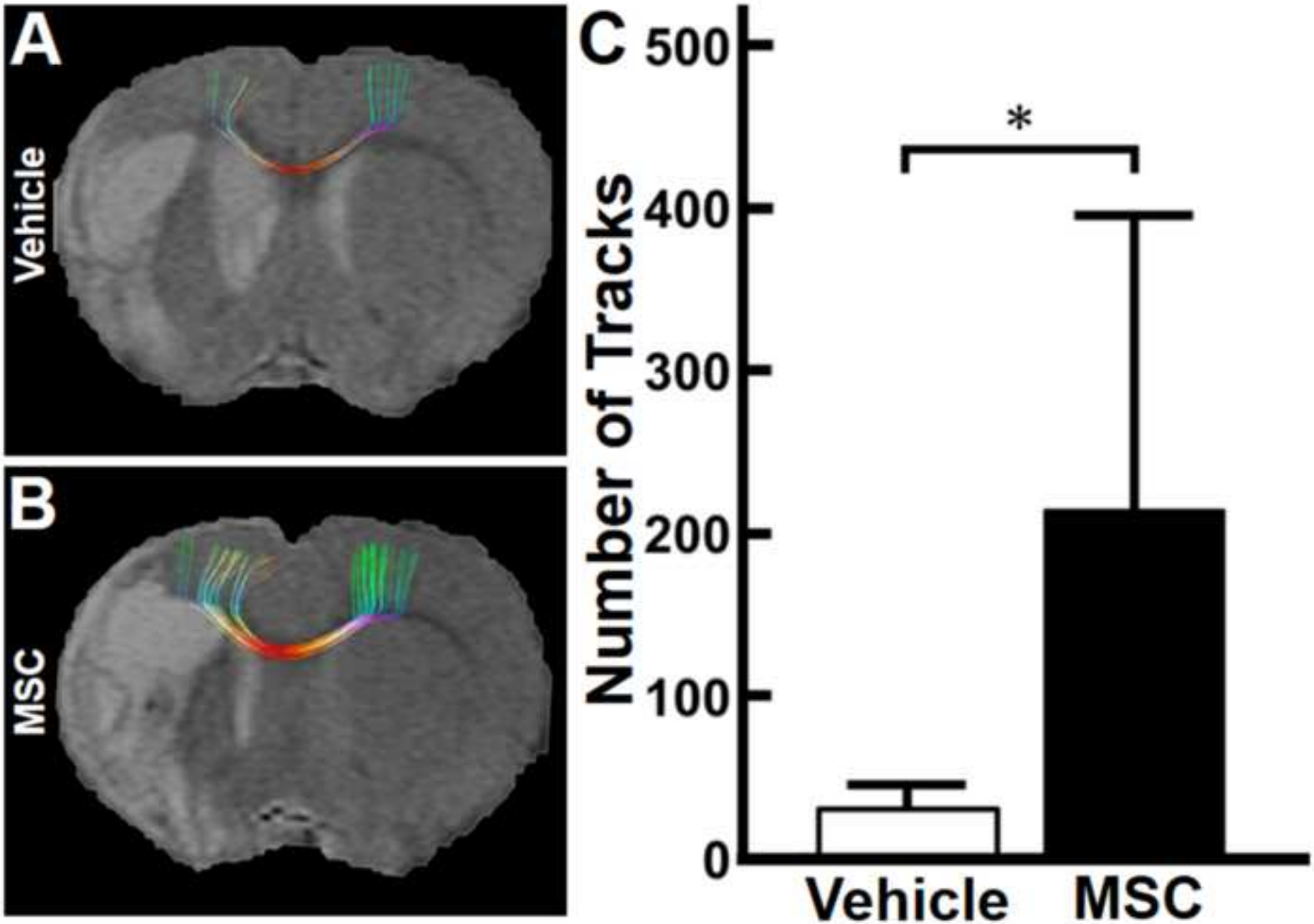

Figure4

Click here to download high resolution image

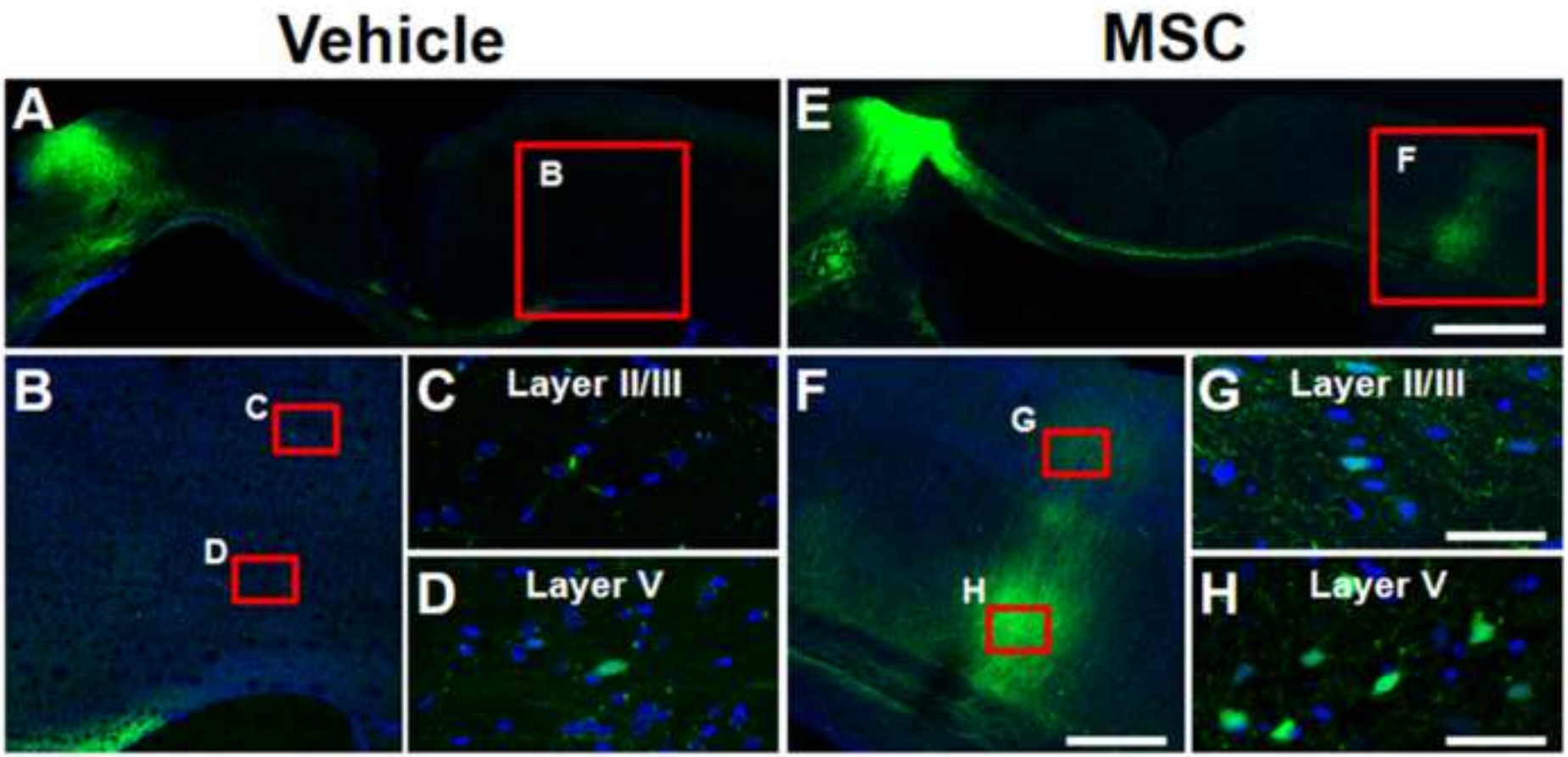

Figure5
Click here to download high resolution image

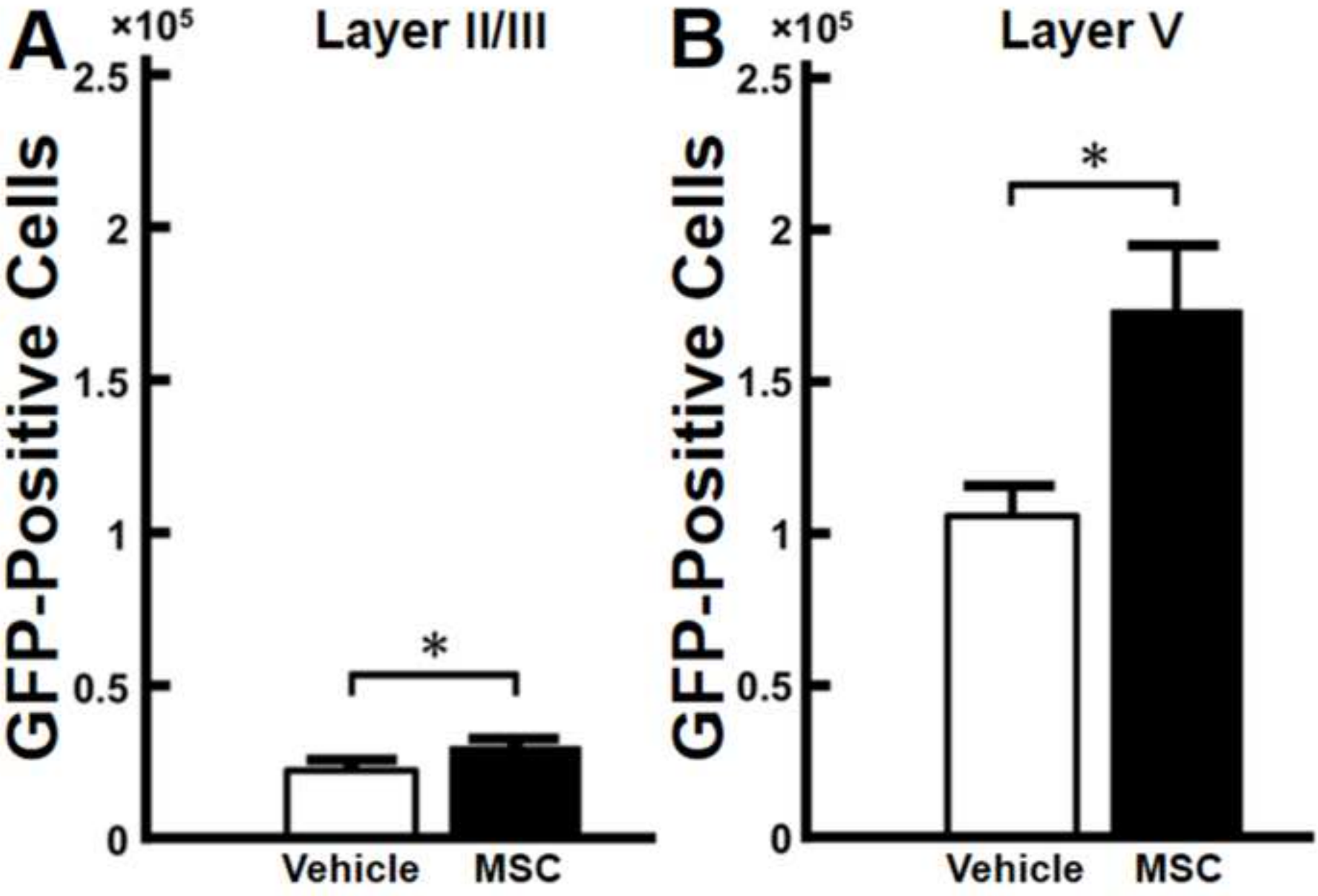

Figure6

Click here to download high resolution image

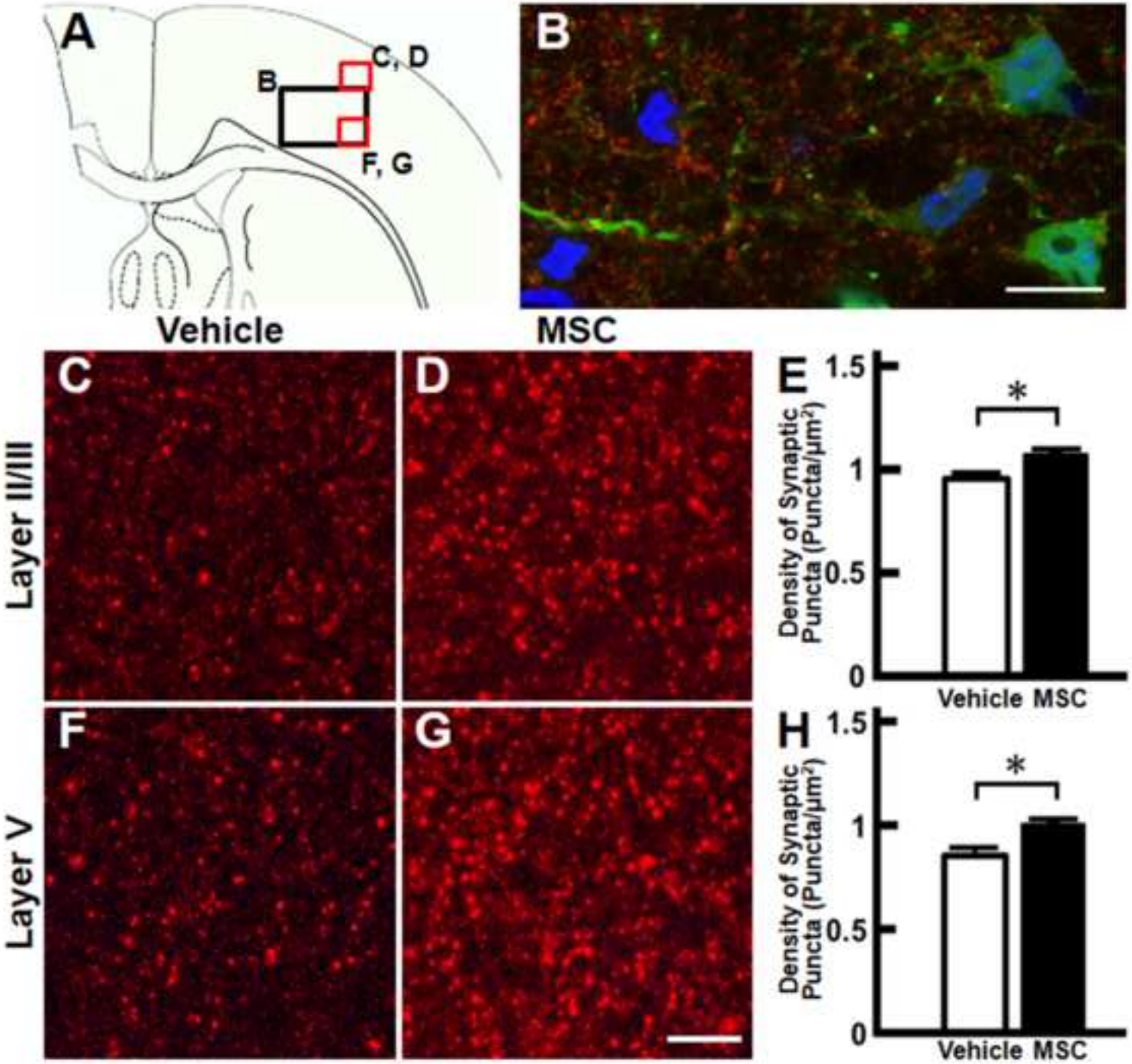

Figure7

Click here to download high resolution image